BMSSM implications for cosmology

JHEP08(2009)053

(http://iopscience.iop.org/1126-6708/2009/08/053)

Published by IOP Publishing for SISSA

Received: *July 16, 2009*
Accepted: *July 19, 2009*
Published: *August 13, 2009*

BMSSM implications for cosmology

Nicolás Bernal,[a] **Kfir Blum,**[b] **Yosef Nir**[b] **and Marta Losada**[c]

[a] *High Energy Physics Group, Dept ECM and Institut de Ciències del Cosmos, Universitat de Barcelona, Av. Diagonal 647, E-08028, Barcelona, Catalonia, Spain*

[b] *Department of Particle Physics, Weizmann Institute of Science, Herzl St., Rehovot 76100, Israel*

[c] *Centro de Investigaciones, Universidad Antonio Nariño, Cra 3 Este No 47A-15, Bogotá, Colombia*

E-mail: bernal@ecm.ub.es, Kfir.Blum@weizmann.ac.il, Yosef.Nir@weizmann.ac.il, malosada@uan.edu.co

Abstract: The addition of non-renormalizable terms involving the Higgs fields to the MSSM (BMSSM) ameliorates the little hierarchy problem of the MSSM. We analyze in detail the two main cosmological issues affected by the BMSSM: dark matter and baryogenesis. The regions for which the relic abundance of the LSP is consistent with WMAP and collider constraints are identified, showing that the bulk region and other previously excluded regions are now permitted. Requiring vacuum stability limits the allowed regions. Based on a two-loop finite temperature effective potential analysis, we show that the electroweak phase transition can be sufficiently first order in regions that for the MSSM are incompatible with the LEP Higgs mass bound, including parameter values of $\tan\beta \lesssim 5$, $m_{\tilde{t}_1} > m_t$, $m_Q \ll \text{TeV}$.

Keywords: Supersymmetry Phenomenology

ArXiv ePrint: 0906.4696

doi:10.1088/1126-6708/2009/08/053

JHEP08(2009)053

Contents

JHEP08(2009)053

1 Introduction

The smallness of the quartic Higgs coupling in the framework of the minimal supersymmetric standard model (MSSM) poses a problem. The tree level bound on the Higgs mass is violated, and large enough loop corrections to satisfy the lower bound on the Higgs mass suggest that the stop sector has rather peculiar features: at least one of the stop mass eigenstates should be rather heavy and/or left-right-stop mixing should be substantial.

The situation is different if the quartic Higgs couplings are affected by new physics. If the new physics appears at an energy scale that is somewhat higher than the electroweak breaking scale, then its effects can be parameterized by non-renormalizable terms. The leading non-renormalizable terms that modify the quartic couplings are [1–7]:

$$W_{\rm BMSSM} = \frac{\lambda_1}{M}(H_u H_d)^2 + \frac{\lambda_2}{M}\mathcal{Z}(H_u H_d)^2, \tag{1.1}$$

where $\mathcal{Z}$ is a SUSY-breaking spurion:

$$\mathcal{Z} = \theta^2 m_{\rm susy}. \tag{1.2}$$

The first term in eq. (1.1) is supersymmetric, while the second breaks supersymmetry (SUSY). In the scalar potential, the following quartic terms are generated:

$$2\epsilon_1 H_u H_d (H_u^\dagger H_u + H_d^\dagger H_d) + \epsilon_2 (H_u H_d)^2, \tag{1.3}$$

where

$$\epsilon_1 \equiv \frac{\mu^* \lambda_1}{M}, \qquad \epsilon_2 \equiv -\frac{m_{\rm susy} \lambda_2}{M}. \tag{1.4}$$

The interplay between the Higgs sector, the stop sector, and the non-renormalizable (NR) operators has interesting consequences for the MSSM baryogenesis [8]. The window for MSSM baryogenesis is extended and, most important, can be made significantly more natural. In addition, these operators have implications for yet another cosmological issue, and that is dark matter [9]. In this work we present an extended analysis of the results for both the electroweak phase transition and the dark matter relic abundance in the BMSSM.

One of the attractive features of the MSSM is the fact that the lightest R-parity-odd particle (LSP) is a natural candidate for being the dark matter particle. Progress in experimentally constraining the MSSM parameter space restricts, however, the regions where the dark matter is quantitatively accounted for to rather special regions of the MSSM: the focus point region, with surprisingly heavy sfermions; the funnel region, where the mass of the CP-odd neutral Higgs scalar is very close to twice the mass of the LSP; the co-annihilation region, where the mass of the scalar partner of the right-handed tau is very close to the mass of the LSP; and the bulk region, where the bino-LSP and the sleptons are light.

The effects of the NR operators are potentially important for two of these four regions. First, these operators give rise to a new Higgs-Higgs-higgsino-higgsino interaction Lagrangian,

$$-\frac{\epsilon_1}{\mu^*}\left[2(H_u H_d)(\widetilde{H}_u \widetilde{H}_d)+2(\widetilde{H}_u H_d)(H_u \widetilde{H}_d)+(H_u \widetilde{H}_d)(H_u \widetilde{H}_d)+(\widetilde{H}_u H_d)(\widetilde{H}_u H_d)\right]+\text{h.c.}, \tag{1.5}$$

which contributes to the annihilation process of two higgsinos to two Higgs particles. This effect is relevant when the dark matter particle has a significant component of higgsinos, as is the case in the focus point region. Second, as mentioned above, these operators modify the relation between the light Higgs mass and the stop masses. This effect can be important in the bulk region within models where the slepton and stop masses are related, such as the mSUGRA models. In this work, we will study these effects and assess their quantitative significance.

The plan of this paper is as follows. In section 2 we present the BMSSM spectra of the Higgs, neutralino and chargino sectors, and the implications for the stop spectrum. In section 3 we describe the BMSSM modifications to the annihilation cross sections that are relevant to the dark matter relic abundance. In section 4 we analyze the implications of the BMSSM operators for dark matter, while in section 5 we explore the parameter space where the electroweak phase transition (EWPT) is strongly first order, as required for successful baryogenesis. We summarize our conclusions in section 6.

2 The spectrum

2.1 The Higgs sector and light stops

We define the scalar Higgs components by

$$H_d = \begin{pmatrix} H_d^0 \\ H_d^- \end{pmatrix} = \begin{pmatrix} \frac{\phi_1 + H_{dr} + i H_{di}}{\sqrt{2}} \\ H_d^- \end{pmatrix}$$

$$H_u = \begin{pmatrix} H_u^+ \\ H_u^0 \end{pmatrix} = \begin{pmatrix} H_u^+ \\ \frac{\phi_2 + H_{ur} + iH_{ui}}{\sqrt{2}} \end{pmatrix}. \tag{2.1}$$

The VEVs of these Higgs fields are parameterized by

$$\begin{aligned} \langle H_d^0 \rangle &= \phi_1/\sqrt{2}, & \langle H_u^0 \rangle &= \phi_2/\sqrt{2}, \\ \tan\beta &= |\phi_2/\phi_1|, & v &= \sqrt{(\phi_1^2 + \phi_2^2)/2} \simeq 174 \text{ GeV}. \end{aligned} \tag{2.2}$$

To leading order, the two charged and four neutral Higgs mass eigenstates are related to the interaction eigenstates via

$$\begin{aligned} \begin{pmatrix} H_d^{*+} \\ H_u^+ \end{pmatrix} &= \begin{pmatrix} s_\beta & -c_\beta \\ c_\beta & s_\beta \end{pmatrix} \begin{pmatrix} H^+ \\ G^+ \end{pmatrix}, \\ \begin{pmatrix} H_{di} \\ H_{ui} \end{pmatrix} &= \begin{pmatrix} s_\beta & -c_\beta \\ c_\beta & s_\beta \end{pmatrix} \begin{pmatrix} A \\ G^0 \end{pmatrix}, \\ \begin{pmatrix} H_{dr} \\ H_{ur} \end{pmatrix} &= \begin{pmatrix} c_\alpha & -s_\alpha \\ s_\alpha & c_\alpha \end{pmatrix} \begin{pmatrix} H \\ h \end{pmatrix}, \end{aligned} \tag{2.3}$$

where $c_\beta \equiv \cos\beta$, $s_\beta \equiv \sin\beta$, and similarly for α. Within the MSSM (without the ϵ_i operators), the angle α is given by (at tree level)

$$s_{2\alpha} = -\frac{m_A^2 + m_Z^2}{m_H^2 - m_h^2}\, s_{2\beta}. \tag{2.4}$$

If the $\epsilon_{1,2}$ couplings are complex, then the four neutral mass eigenstates are related by a 4×4 transformation matrix to the real and imaginary components of H_d^0 and H_u^0. The analysis of dark matter is, however, unaffected at leading order, so we neglect such effects here. In the unitary gauge, the Goldstone fields $G^\pm$ and G^0 are set to zero.

Taking m_Z, m_A and $\tan\beta$ as input parameters, we obtain the following ϵ_i-corrections to the Higgs spectrum:

$$\begin{aligned} \delta_\epsilon m_h^2 &= 2v^2 \left(\epsilon_{2r} - 2\epsilon_{1r} s_{2\beta} - \frac{2\epsilon_{1r}(m_A^2 + m_Z^2)s_{2\beta} + \epsilon_{2r}(m_A^2 - m_Z^2)c_{2\beta}^2}{\sqrt{(m_A^2 - m_Z^2)^2 + 4m_A^2 m_Z^2 s_{2\beta}^2}} \right), \\ \delta_\epsilon m_H^2 &= 2v^2 \left(\epsilon_{2r} - 2\epsilon_{1r} s_{2\beta} + \frac{2\epsilon_{1r}(m_A^2 + m_Z^2)s_{2\beta} + \epsilon_{2r}(m_A^2 - m_Z^2)c_{2\beta}^2}{\sqrt{(m_A^2 - m_Z^2)^2 + 4m_A^2 m_Z^2 s_{2\beta}^2}} \right), \\ \delta_\epsilon m_{H^\pm}^2 &= 2v^2 \epsilon_{2r}. \end{aligned} \tag{2.5}$$

The angle α is shifted from its MSSM value:

$$\begin{aligned} s_{2\alpha} &= \frac{-(m_A^2 + m_Z^2)s_{2\beta} + 4v^2\epsilon_{1r}}{(m_H^2 - m_h^2)s_{2\beta}} \\ &= -\frac{(m_A^2 + m_Z^2)s_{2\beta}}{(m_A^4 - 2m_A^2 m_Z^2 c_{4\beta} + m_Z^4)^{1/2}} - 4v^2 c_{2\beta}^2 \frac{2\epsilon_{1r}(m_A^2 - m_Z^2)^2 - \epsilon_{2r} s_{2\beta}(m_A^4 - m_Z^4)}{(m_A^4 - 2m_A^2 m_Z^2 c_{4\beta} + m_Z^4)^{3/2}}. \end{aligned} \tag{2.6}$$

The possibility of a light Higgs scalar hidden in the LEP data is not excluded (see e.g. [10]) and, in fact, may have interesting implications for DM [11]. This scenario relies upon sizable mixing in the Higgs mass matrix, such that production via $e^+e^- \to Zh$ is suppressed. Hence the mass splitting in the scalar Higgs sector must be rather small. A light Higgs sector is an interesting possibility also within the BMSSM, following the impact of the non-renormalizable operators on the mixing angles, captured to leading order in eq. (2.6). An extreme example for this possibility was presented in [6], in which the electroweak symmetry breaking vacuum is controlled by the non-renormalizable operators.

In the present work, we limit our attention to the more conservative situation wherein the non-renormalizable operators can still be treated as perturbations in the usual electroweak breaking vacuum of the MSSM. We allow for significant splitting between the heavy and light Higgs mass eigenstates, in which case the constraint that arises from the LEP bound on the light Higgs mass can be written as follows:

$$m_h^2 \approx m_h^{2(\text{tree})} + \delta_t m_h^2 + \delta_\epsilon m_h^2 \gtrsim \left(114 \text{ GeV}\right)^2, \tag{2.7}$$

where

$$\begin{aligned}
\delta_t m_h^2 &= \frac{3m_t^4}{4\pi^2 v^2} \ln\left(\frac{m_{\tilde{t}_1} m_{\tilde{t}_2}}{m_t^2}\right) \\
&\quad + \frac{3m_t^4}{4\pi^2 v^2} \frac{|X_t|^2}{m_{\tilde{t}_1}^2 - m_{\tilde{t}_2}^2} \left[\ln\left(\frac{m_{\tilde{t}_1}^2}{m_{\tilde{t}_2}^2}\right) + \frac{1}{2}\frac{|X_t|^2}{m_{\tilde{t}_1}^2 - m_{\tilde{t}_2}^2}\left(2 - \frac{m_{\tilde{t}_1}^2 + m_{\tilde{t}_2}^2}{m_{\tilde{t}_1}^2 - m_{\tilde{t}_2}^2} \ln\left(\frac{m_{\tilde{t}_1}^2}{m_{\tilde{t}_2}^2}\right)\right)\right], \\
X_t &= A_t + \mu^* \cot\beta.
\end{aligned} \tag{2.8}$$

The $\delta_\epsilon m_h^2$ contribution relaxes the constraints on $\delta_t m_h^2$ in a significant way. In fact, $\delta_t m_h^2 \leq 0$ is not excluded (in this respect we disagree with the conclusions of [7]). Thus, for $\epsilon_1 \lesssim -0.05$ and $\tan\beta \lesssim 10$, the two stop mass eigenstates can be as light as the top quark, or one could be as light as the direct experimental lower bound with the other only slightly heavier than the top.

2.2 Neutralinos

The neutralino mass matrix is given by

$$M_{\tilde{N}} = \begin{pmatrix} M_1 & 0 & -m_Z s_W c_\beta & m_Z s_W s_\beta \\ 0 & M_2 & m_Z c_W c_\beta & -m_Z c_W s_\beta \\ -m_Z s_W c_\beta & m_Z c_W c_\beta & 0 & -\mu \\ m_Z s_W s_\beta & -m_Z c_W s_\beta & -\mu & 0 \end{pmatrix} + \frac{4\epsilon_1 m_W^2}{\mu^* g^2} \begin{pmatrix} 0 & 0 & 0 & 0 \\ 0 & 0 & 0 & 0 \\ 0 & 0 & s_\beta^2 & s_{2\beta} \\ 0 & 0 & s_{2\beta} & c_\beta^2 \end{pmatrix}. \tag{2.9}$$

The transition to the neutralino mass basis is obtained with a unitary matrix Z:

$$M_{\tilde{N}} = Z^T \text{ diag}(m_{\tilde{N}_1}, m_{\tilde{N}_2}, m_{\tilde{N}_3}, m_{\tilde{N}_4})\ Z. \tag{2.10}$$

The gaugino fraction in the LSP is defined as

$$R_{\tilde{\lambda}} = |Z_{11}|^2 + |Z_{12}|^2, \tag{2.11}$$

while the higgsino fraction is given by $1 - R_{\tilde{\lambda}} = |Z_{13}|^2 + |Z_{14}|^2$.

JHEP08(2009)053

2.3 Charginos

The chargino mass matrix is given by

$$M_{\widetilde{C}} = \begin{pmatrix} M_2 & \sqrt{2} m_W s_\beta \\ \sqrt{2} m_W c_\beta & \mu \end{pmatrix} - \frac{2\epsilon_1 m_W^2 s_{2\beta}}{\mu^* g^2} \begin{pmatrix} 0 & 0 \\ 0 & 1 \end{pmatrix}. \tag{2.12}$$

The transition to the neutralino mass basis is obtained with unitary matrices V and U:

$$M_{\widetilde{C}} = U^T \ \mathrm{diag}(m_{\widetilde{C}_1}, m_{\widetilde{C}_2}) \ V. \tag{2.13}$$

3 Annihilation cross sections

The effects of the BMSSM operators on (co)annihilation cross sections are relevant to the dark matter issue when the LSP has a significant component of higgsino, namely $1 - R_{\tilde{\lambda}} \not\ll 1$. These effects come in two ways. First, there is an indirect effect, due to the modification of the neutralino and chargino spectra. Since co-annihilation rates are very sensitive to mass splittings, this is often the more important effect. Second, there is a direct effect of the new ϵ_1-dependent couplings which modify the (co)annihilation processes that involve Higgs scalars as mediators and/or as final states. In this section, we focus on the latter effect. In section 4 we analyze numerically the DM relic abundance in the BMSSM, taking into account all effects.

3.1 Single scalar

We consider terms of the form

$$C_\phi \phi \overline{\tilde{N}} \tilde{N}; \qquad C_\phi \phi \overline{\tilde{N}} \tilde{C}^+, \qquad \phi = h, H, A; H^-. \tag{3.1}$$

We denote the MSSM couplings by C_ϕ^0 and define the modification that is induced by the ϵ_1 terms as follows:

$$C_\phi = C_\phi^0 (1 - \delta_{\epsilon\phi}). \tag{3.2}$$

As concerns the emission of a single neutral scalar in the annihilation of two neutralino LSPs, we obtain the following $\delta_{\epsilon\phi}$'s:

$$\delta_{\epsilon h} = \frac{2\sqrt{2}\lambda_1^* v}{gM} \times \frac{-c_\beta s_\alpha Z_{14}^2 + s_\beta c_\alpha Z_{13}^2 + 2 c_{(\alpha+\beta)} Z_{13} Z_{14}}{(Z_{12} - \tan\theta_W Z_{11})(s_\alpha Z_{13} + c_\alpha Z_{14})}, \tag{3.3}$$

$$\delta_{\epsilon H} = \frac{2\sqrt{2}\lambda_1^* v}{gM} \times \frac{c_\beta c_\alpha Z_{14}^2 + s_\beta s_\alpha Z_{13}^2 + 2 s_{(\alpha+\beta)} Z_{13} Z_{14}}{(Z_{12} - \tan\theta_W Z_{11})(-c_\alpha Z_{13} + s_\alpha Z_{14})}, \tag{3.4}$$

$$\delta_{\epsilon A} = \frac{\sqrt{2}\lambda_1^* v}{gM} \times \frac{s_{2\beta}(Z_{14}^2 + Z_{13}^2) + 4 Z_{13} Z_{14}}{(Z_{12} - \tan\theta_W Z_{11})(s_\beta Z_{13} - c_\beta Z_{14})}. \tag{3.5}$$

As concerns the emission of a single charged scalar in the co-annihilation of the neutralino LSP with the lightest chargino, we obtain the following $\delta_{\epsilon H^-}$'s:

$$\delta_{\epsilon H^- R} = \frac{2\lambda_1^* v}{gM \tan\beta} \times \frac{U_{12}(c_\beta Z_{14} + s_\beta Z_{13})}{U_{11} Z_{13} - \frac{1}{\sqrt{2}} U_{12}(Z_{12} + \tan\theta_W Z_{11})}, \tag{3.6}$$

$$\delta^*_{\epsilon H^- L} = \frac{2\lambda_1^* v \tan\beta}{gM} \times \frac{V_{12}(c_\beta Z_{14} + s_\beta Z_{13})}{V_{11} Z_{14} + \frac{1}{\sqrt{2}} V_{12}(Z_{12} + \tan\theta_W Z_{11})}. \tag{3.7}$$

The R and L sub-indices correspond to P_R and P_L which project a Dirac higgsino onto the lower and upper Weyl fermion, respectively. Thus, $C_{H^- R}$ is the coupling of the $H^- \overline{\widetilde{N}} P_R \widetilde{C}^+$ term, while $C^*_{H^- L}$ is the coupling of the $H^- \overline{\widetilde{N}} P_L \widetilde{C}^+$ term.

To get some intuition about the expected size of the correction to the MSSM annihilation cross section, we can estimate from the above expressions that the relative size of the correction, κ:

$$\kappa \sim 0.1 \left(\frac{5 \text{ TeV}}{M/\lambda_1}\right) \left(\frac{1 - R_{\tilde{\lambda}}}{0.1}\right)^{1/2}. \tag{3.8}$$

Thus, if there is a new physics threshold at around 5 TeV, and the higgsino component in the LSP is of order ten percent, then the correction to the annihilation cross section is of order ten percent. To make contact with the scalar spectrum, it is also useful to represent eq. (3.8) in terms of ϵ_1 and μ,

$$\kappa \sim 0.6 \left(\frac{m_W}{\mu}\right) \left(\frac{\epsilon_1}{0.1}\right) \left(\frac{1 - R_{\tilde{\lambda}}}{0.1}\right)^{1/2}. \tag{3.9}$$

As the new physics threshold scales like $\sim \mu/\epsilon_1$, it is difficult to envisage a phenomenologically acceptable scenario exhibiting $\mu \sim m_W$ simultaneously with $\epsilon_1 \sim 0.1$. Hence some suppression is to be expected from the combination of mass and ϵ factors in (3.9). This implies that the BMSSM modification to the relevant MSSM annihilation processes is at most of $\mathcal{O}(10\%)$ in generic cases.

3.2 Two scalars

We consider terms of the form

$$\overline{\tilde{N}_1}(y^r_{ab} + i y^i_{ab}\gamma^5)\tilde{N}_1 \phi_a \phi_b, \tag{3.10}$$

where y_{ab} has mass dimension of -1. Keeping only potential s- and p-wave contributions, we obtain for the annihilation cross section into $\phi_a \phi_b$:

$$\sigma_{ab} v = \frac{\bar{\beta}_f c^2_{ab} m^2_{\tilde{N}_1}}{4\pi S} \left[(y^i_{ab})^2 + \frac{v^2}{4} \left((y^r_{ab})^2 + \frac{3}{2}(y^i_{ab})^2 \right) \right], \tag{3.11}$$

where $m_{\tilde{N}_1}$ is the LSP mass, $c_{ab} = 2(1 + \delta_{ab})$, S is the center-of-mass energy squared,

$$S \approx 4 m^2_{\tilde{N}_1}(1 + v^2/4), \tag{3.12}$$

and

$$\bar{\beta}_f \equiv \frac{2|\vec{p}_a|}{\sqrt{S}} \approx \sqrt{1 + \frac{(m_a - m_b)^2}{16 m^4_{\tilde{N}_1}} - \frac{m_a^2 + m_b^2}{2 m^2_{\tilde{N}_1}}}. \tag{3.13}$$

In terms of the Lagrangian parameters, we have

$$\begin{aligned} y^r_{ab} &= -\frac{1}{2M} \mathcal{R}e\left(\lambda_1^* Y_{ab}\right), \quad y^i_{ab} = -\frac{1}{2M} \mathcal{I}m\left(\lambda_1^* Y_{ab}\right), \quad \phi_a \phi_b = hh, HH, AA, hH, H^+H^- \\ y^r_{ab} &= \frac{1}{2M} \mathcal{I}m\left(\lambda_1^* Y_{ab}\right), \quad y^i_{ab} = -\frac{1}{2M} \mathcal{R}e\left(\lambda_1^* Y_{ab}\right), \quad \phi_a \phi_b = hA, HA. \end{aligned} \tag{3.14}$$

JHEP08(2009)053

The dimensionless Y_{ab} couplings are given by

$$\begin{aligned}
Y_{hh} &= s_\alpha^2 Z_{14}^2 + c_\alpha^2 Z_{13}^2 - 2 s_{2\alpha} Z_{14} Z_{13}, \\
Y_{HH} &= c_\alpha^2 Z_{14}^2 + s_\alpha^2 Z_{13}^2 + 2 s_{2\alpha} Z_{14} Z_{13}, \\
Y_{AA} &= -s_\beta^2 Z_{14}^2 - c_\beta^2 Z_{13}^2 - 2 s_{2\beta} Z_{14} Z_{13}, \\
Y_{hH} &= s_{2\alpha}(-Z_{14}^2 + Z_{13}^2) + 4 c_{2\alpha} Z_{14} Z_{13}, \\
Y_{hA} &= 2 s_\alpha s_\beta Z_{14}^2 - 2 c_\alpha c_\beta Z_{13}^2 + 4 s_{(\alpha-\beta)} Z_{14} Z_{13}, \\
Y_{HA} &= -2 c_\alpha s_\beta Z_{14}^2 - 2 s_\alpha c_\beta Z_{13}^2 - 4 c_{(\alpha-\beta)} Z_{14} Z_{13}, \\
Y_{H^+H^-} &= -2 s_{2\beta} Z_{13} Z_{14}.
\end{aligned} \tag{3.15}$$

Co-annihilation proceeds via terms of the form

$$\overline{\tilde{N}_1}(y^e_{ab} + y^o_{ab}\gamma^5)\tilde{C}_1^+, \tag{3.16}$$

with y^e, y^o complex. The cross-section is given by an expression similar to eq. (3.11), provided that the neutralino-chargino mass difference is neglected, taking $c_{ab} = 1$, and making the substitution $(y^r)^2 \to |y^e|^2$, $(y^i)^2 \to |y^o|^2$. We now have

$$\begin{aligned}
y^{e,o}_{H^-\phi_b} &= -\frac{1}{2M}\left(\lambda_1^* Y_{H^-\phi_b R} \pm \lambda_1 Y^*_{H^-\phi_b L}\right), \qquad \phi_b = h, H, \\
y^{e,o}_{H^-A} &= -\frac{1}{2M}\left(\lambda_1^* Y_{H^-AR} \mp \lambda_1 Y^*_{H^-AL}\right),
\end{aligned} \tag{3.17}$$

$$\begin{aligned}
Y_{H^-hR} &= \sqrt{2} c_\beta U_{12}(s_\alpha Z_{14} - c_\alpha Z_{13}), \\
Y_{H^-hL} &= \sqrt{2} s_\beta V_{12}(s_\alpha Z_{14} - c_\alpha Z_{13}), \\
Y_{H^-HR} &= -\sqrt{2} c_\beta U_{12}(c_\alpha Z_{14} + s_\alpha Z_{13}), \\
Y_{H^-HL} &= -\sqrt{2} s_\beta V_{12}(c_\alpha Z_{14} + s_\alpha Z_{13}), \\
Y_{H^-AR} &= \sqrt{2} c_\beta U_{12}(s_\beta Z_{14} + c_\beta Z_{13}), \\
Y_{H^-AL} &= \sqrt{2} s_\beta V_{12}(s_\beta Z_{14} + c_\beta Z_{13}).
\end{aligned} \tag{3.18}$$

To get some intuition about the expected size of the correction to the MSSM annihilation cross section, let us consider the case of a higgsino LSP, $R_{\tilde{\lambda}} \approx 0$, wherein the couplings (3.15) and (3.18) are unsuppressed. In the MSSM, annihilation into (mostly transverse) gauge bosons gives $\langle\sigma v\rangle \sim \frac{g^4}{85\pi\mu^2}$ [12]. Regarding the BMSSM contribution (3.11) to annihilation into light Higgs boson pairs, we obtain $\langle\sigma v\rangle \sim \frac{\lambda_1^2}{24\pi M^2}$. This estimate holds when there is no CP violation and the leading contribution is p-wave. Writing the modified cross section as $\langle\sigma v\rangle = \langle\sigma v\rangle_0(1+\delta_\epsilon)$, we find $\delta_\epsilon \sim 0.25\left(\frac{\epsilon_1}{0.1}\right)^2$. Note, however, that in the relevant scenario co-annihilations are important and so further numerical study is required to assess the full impact of the BMSSM. Below, we proceed to perform this study.

4 The dark matter relic density

As deduced from the WMAP satellite measurement of the temperature anisotropies in the Cosmic Microwave Background, cold dark matter makes up approximately 23% of the

JHEP08(2009)053

energy of the Universe [13]. The DM cosmological density is precisely measured to be

$$\Omega_{DM}\, h^2 = 0.101 \pm 0.0062 \tag{4.1}$$

at 68% CL. The accuracy is expected to be improved to the percent level by future measurements at Planck satellite [14].

We calculate the dark matter relic density in the presence of the ϵ_1 couplings using a modified version of the code MicrOMEGAs [15], where we implemented the BMSSM Higgs-Higgs-higgsino-higgsino couplings of eq. (1.5). The leading $\epsilon_{1,2}$-induced corrections to the MSSM Higgs spectrum, eq. (2.5), were implemented using the code SuSpect [16].

The BMSSM framework, if relevant to the little hierarchy problem that arises from the lower bound on the Higgs mass, assumes a new physics scale at a few TeV. Since the new degrees of freedom at this scale are not specified, the effect of the new threshold on the running of parameters from a much higher scale cannot be rigorously taken into account. It therefore only makes sense to study the BMSSM effects in a framework specified at low energy. In order to demonstrate some of the most interesting consequences of the BMSSM operators for dark matter, we will employ two such sets of parameters: a model where all sfermion masses are correlated, and a model where the only light sfermions are the stops. The first model demonstrates how the so-called bulk region is re-opened, even for correlated stop and slepton masses. The second model incorporates the interesting process of stop co-annihilation. For both models we focus our attention mainly on regions where the stops are light, since the main motivation for the BMSSM operators is to avoid a heavy stop (which is the cause of the little hierarchy problem) and, furthermore, this is the region that is relevant to BMSSM baryogenesis. Previous analysis in the context of the MSSM with a light stop were done in [17–19].

4.1 Correlated stop-slepton masses

The most natural dark matter scenario within the MSSM framework could have been that of a light bino, annihilating to the standard model leptons via light slepton exchange. This scenario is known as the "bulk region" of the MSSM. However, in some of the most intensively studied MSSM scenarios, such as the mSUGRA [20] or cMSSM frameworks, the part of the bulk region that is allowed became smaller and smaller as the experimental lower bound on the Higgs mass became stronger. The generic reason for this is that a stronger lower bound on the Higgs mass requires a heavier stop which, in these frameworks, further implies heavy sleptons. One way to re-open the bulk region is to assume a framework where the stop and the slepton masses are not correlated. The BMSSM, however, re-opens the bulk region in a different way: the stop is not required to be heavy anymore.

In order to understand these implications of the BMSSM framework and, in particular, in order to allow for a simple comparison with mSUGRA-like models, we investigate the following framework. The MSSM parameters that we use are those that would have corresponded to an mSUGRA model specified by the five parameters

$$\tan\beta,\ m_{1/2},\ m_0,\ A_0,\ \mathrm{sign}(\mu). \tag{4.2}$$

JHEP08(2009)053

Thus, the correlations between the low energy MSSM parameters are the same as those that would hold in an mSUGRA framework. In other words, our low energy parameters are expressed in terms of the parameters in (4.2) approximately as follows [21]:

$$\begin{aligned} m^2_{\tilde{q}} &\approx m_0^2 + 6\, m_{1/2}^2, \\ m^2_{\tilde{\ell}_L} &\approx m_0^2 + 0.5\, m_{1/2}^2, \\ m^2_{\tilde{\ell}_R} &\approx m_0^2 + 0.15\, m_{1/2}^2, \\ M_1 &\approx 0.4\, m_{1/2}, \\ M_2 &\approx 0.8\, m_{1/2}, \\ M_3 &\approx 3\, m_{1/2}. \end{aligned} \tag{4.3}$$

The values of μ^2 and m_A^2 depend on the soft breaking terms and on the electroweak breaking parameters in the standard way. Let us emphasize again that one should *not* think about this set of parameters as coming from an extended mSUGRA model, since the effects of the BMSSM physics at the few TeV scale on the running are not (and cannot) be taken into account. In addition, we have two extra BMSSM parameters: ϵ_1 and ϵ_2. We focus essentially on the effects of ϵ_1.

In practice, we make discrete choices of $\tan\beta$, A_0, $\mathrm{sign}(\mu)$ and ϵ_1, and scan over m_0 and $m_{1/2}$. We focus our attention on moderate values of $m_{1/2}$ and m_0 because we are mainly interested in light sfermions and the bulk region. Figure 1 displays the area, in the $[m_0, m_{1/2}]$ plane, where the WMAP constraint is satisfied (between the solid red lines). We use $A_0 = 0\,\mathrm{GeV}$, $\mu > 0$, and values of $\tan\beta$, ϵ_1 and ϵ_2 as indicated in the various plots. The region below the dotted blue curve is excluded by the null searches for charginos and sleptons at LEP. The area to the left and above the orange curve is excluded because the stau is the LSP. The dotted black curves are contour lines for m_h.

We would like to emphasize several points regarding the effects that are demonstrated by figure 1:

1. The most significant effect of the BMSSM operators is their impact on the Higgs boson mass. Within the MSSM with mSUGRA-like correlations, the bound on the Higgs mass strongly constrains $m_{1/2}$. In contrast, in the presence of $\epsilon_1 = \mathcal{O}(-0.05)$, the full region for which the correct value of the relic abundance is obtained is allowed.

2. Another significant effect is the appearance (for negative enough ϵ_1 values) of a new region fulfilling the DM constraint. This is the 'h-pole' region in which $m_h \sim 2\, m_{\chi_1^0}$, and the s-channel Higgs exchange is nearly resonant, allowing the neutralinos to annihilate efficiently [22].

3. For the case discussed in this subsection, the co-annihilation region with the stops is not present as the mass difference with the LSP is always too large.

4. In the m_0 region that we are considering here, the impact of the BMSSM operators on the mass of the neutralino LSP and on the region fulfilling the WMAP constraint is rather limited. The reason is that in the bulk region the LSP is mostly bino-like, while the BMSSM operators affect the higgsino parameters.

JHEP08(2009)053

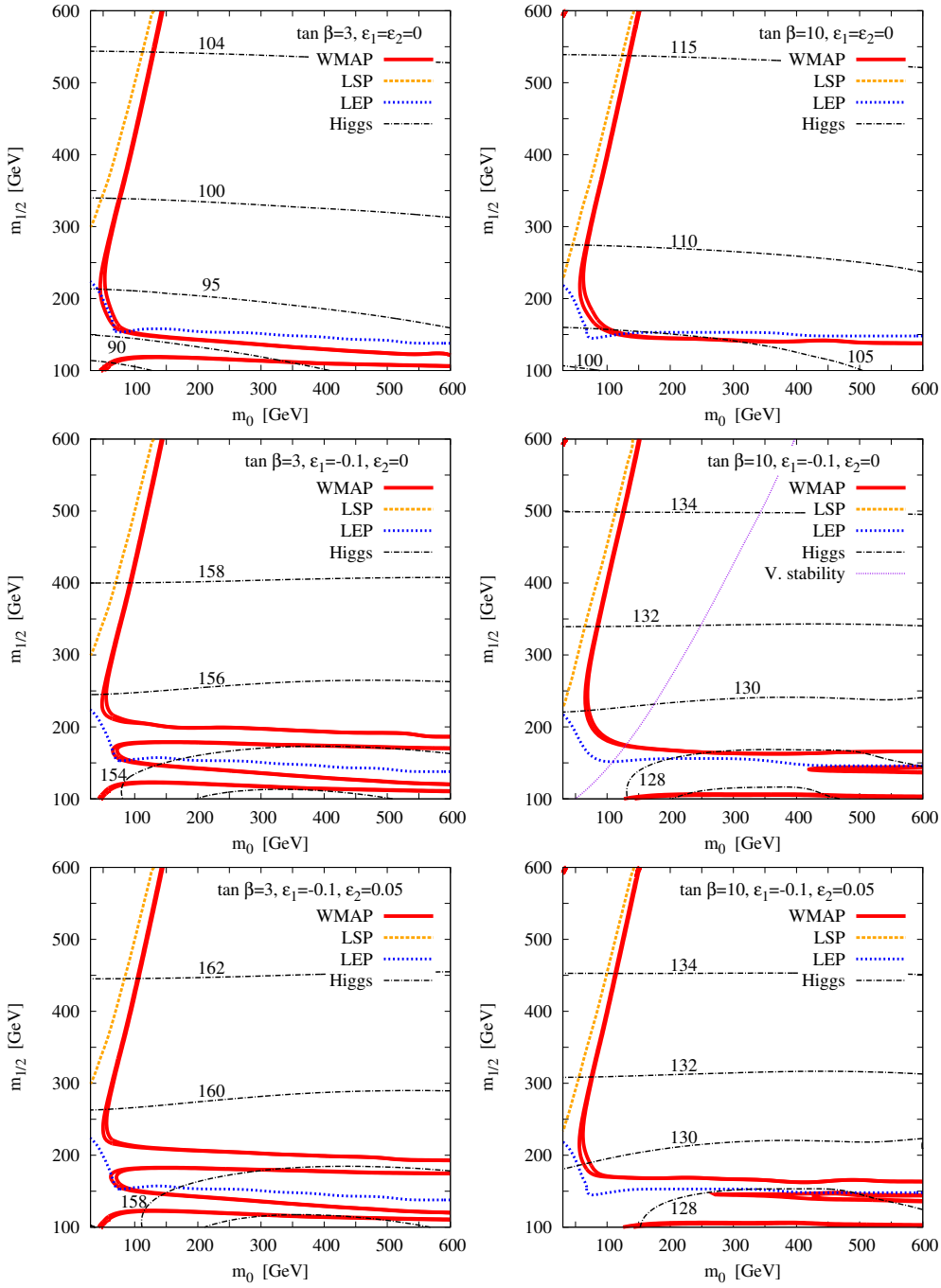

Figure 1. Regions in the $[m_0, m_{1/2}]$ plane in which the WMAP constraint is fulfilled (between the solid red lines). We use $A_0 = 0\,\text{GeV}$, $\mu > 0$, and values of $\tan\beta$, ϵ_1 and ϵ_2 as indicated in the various panels. The region below the dotted blue curve is excluded by the null searches for charginos and sleptons at LEP. The area to the left and above the orange curve is excluded because the stau is the LSP. The dash-dotted black curves are contour lines for m_h with values in GeV as indicated. The dotted purple line in the middle right panel denotes the appearance of a remote vacuum in the scalar potential. Above and to the left of this line, the electroweak vacuum is metastable.

JHEP08(2009)053

The BMSSM operators may destabilize the scalar potential. If $4|\epsilon_1| > \epsilon_2$, the effective quartic coupling along one of the D-flat directions is negative, causing a remote vacuum to form in the presence of which the electroweak vacuum could become metastable. When considering values of $\epsilon_1 \gtrsim -0.1$, vacuum stability is ensured provided that the following condition is fulfilled [23]:

$$\frac{m_A^2}{|\mu|^2} \geq \frac{2}{1+\sin 2\beta}\left(1+\frac{\epsilon_2}{4\epsilon_1}\right)^2 . \tag{4.4}$$

The stability criterion as written here applies when $m_A \gtrsim 3m_Z$. The fact that this criterion involves electroweak scale parameters, and only ratios of non-renormalizable operators, is reminiscent of the supersymmetric origins of ϵ_1. In regions of the parameter space where eq. (4.4) is violated, the electroweak vacuum is metastable. For large $\tan\beta$, this occurs throughout an important fraction of the $[m_0, m_{1/2}]$ plane, depicted in the middle right panel of figure 1 by the area above and to the left of the dotted purple line.

It is important to stress that eq. (4.4) represents an analytical tree level approximation and as such, in the current framework where quantum corrections are sizeable, it is conservative. In order to determine whether the lifetime of the electroweak vacuum is long enough, the rate of quantum tunneling into the remote vacuum should be compared to the Hubble rate. For illustration, consider the two parameter points, P_1 : $[m_0 = 200\ \text{GeV}, m_{1/2} = 150\ \text{GeV}]$ and P_2 : $[m_0 = 100\ \text{GeV}, m_{1/2} = 250\ \text{GeV}]$, with $\tan\beta = 10, \epsilon_1 = -0.1, \epsilon_2 = 0$, as in the middle right panel of figure 1. Point P_1 corresponds to a stable electroweak vacuum configuration, in agreement with the criterion (4.4). Point P_2, on the other hand, violates eq. (4.4) by $\sim 15\%$. However, P_2 involves significant quantum corrections due to stops ($m_{\tilde{t}_1} = 415\,\text{GeV}$, $m_{\tilde{t}_2} = 590\,\text{GeV}$, $A_t = -480\,\text{GeV}$). Calculating the tunneling action, we find that P_2 is in fact long-lived enough to provide an acceptable model point. Similar calculations reveal that the rest of the middle right panel is also long-lived enough (at least marginally), and so eq. (4.4) can not be used to exclude regions in the mSUGRA-like parameter space considered in this section. We will return to the issue of vacuum stability in section 4.2. There, quantum corrections due to stops will be held moderate and fixed, resulting with precise application of eq. (4.4) to exclude significant portions of the parameter space.

As concerns precision electroweak data and low energy processes, it is important to realize that the new physics that generates the non-renormalizable operators can directly modify the constraints that come from these measurements. Ignoring this point, it is still possible to identify regions in the parameter space favored by the WMAP data which satisfy all such low energy constraints. The relevance of the BMSSM lies in the fact that constraints involving the Higgs are decoupled from constraints involving the stop sector. In particular, stops that are neither heavy nor mixed are acceptable, as demonstrated by our choice of $A_0 = 0$ throughout the current section. In contrast, in the case of the MSSM, satisfying the Higgs mass bound as well as electroweak precision data necessitates large values for A_0 [24].

4.2 Light stops, heavy sleptons

The aim of this section is to further expose various implications of the BMSSM for the DM relic abundance, putting special emphasis on parameter regions compatible with a strong first order electroweak phase transition, as required for baryogenesis. In particular, we are

JHEP08(2009)053

interested in the scenario of light, unmixed stops. As mentioned above, LSP co-annihilation with stops is not a viable possibility if the low energy soft supersymmetry breaking parameters obey relations similar to those that would follow from mSUGRA-like theory, unless stop mixing is very large. To explore this possibility in the BMSSM, we employ a set of low energy parameters that is different from the previous subsection. Explicitly, in addition to the BMSSM ϵ_i parameters, we consider the following set of parameters:

$$M_2,\ \mu,\ \tan\beta,\ X_t,\ m_U,\ m_Q,\ m_{\tilde{f}},\ m_A, \tag{4.5}$$

where $m_{\tilde{f}}$ is a common mass for the sleptons, the first and second generation squarks, and $\tilde{b}_R$. We further use $M_1 = \frac{5}{3}\tan^2\theta_W M_2 \sim \frac{1}{2}M_2$.

To demonstrate our main points, we fix the values of all but two parameters as follows: $\epsilon_1 = 0$ or -0.1, $\epsilon_2 = 0$ or $+0.05$, $\tan\beta = 3$ or 10, $X_t = 0$, $m_U = 210\,\text{GeV}$, $m_Q = 400\,\text{GeV}$, $m_{\tilde{f}} = m_A = 500\,\text{GeV}$. This scenario gives rise to relatively light stops:

$$m_{\tilde{t}_1} \lesssim 150\ \text{GeV}, \qquad 370\ \text{GeV} \lesssim m_{\tilde{t}_2} \lesssim 400\ \text{GeV}. \tag{4.6}$$

We scan over the remaining two parameters, M_2 and μ.

In the prescribed framework, one can identify four regions in which the WMAP constraint is fulfilled:

- The 'Z-pole' region in which the LSP is very light, $m_{\chi_1^0} \sim \frac{1}{2}M_Z \sim 45\,\text{GeV}$, and the s-channel Z exchange is nearly resonant. This region is not ruled out only in scenarios where the mass splitting between M_1 and M_2 at the electroweak scale is very large.

- The 'h-pole' region in which the LSP is rather light, $m_{\chi_1^0} \sim \frac{1}{2}M_h$, and the s-channel h exchange is nearly resonant, allowing the neutralinos to annihilate efficiently [22].

- The 'mixed region' in which the LSP is a higgsino-bino mixture [12], $M_2 \sim 2\mu$, which enhances (but not too much) its annihilation cross-sections into final states containing gauge and/or Higgs bosons: $\chi_1^0\chi_1^0 \to W^+W^-$, ZZ, Zh and hh.

- The 'stop co-annihilation' region, in which the LSP is almost degenerate in mass with the lightest stop ($\tilde{t}_1$). Such a scenario leads to an enhanced annihilation of sparticles since the $\chi_1^0 - \tilde{t}_1$ co-annihilation cross-section [25, 26] is much larger than that of the LSP.

Figure 2 displays the areas, in the $[M_2,\ \mu]$ plane, in which the WMAP constraint is satisfied (between the solid red lines). The region of large μ and M_2, to the right of the orange dashed line, is excluded since the lightest stop becomes the LSP. The region of small μ and/or M_2, below and to the left of the blue dotted line, is excluded by the null search for charginos at LEP2 [27].

Let us first consider the two upper panels, where $\epsilon_1 = \epsilon_2 = 0$. The various regions described above that are consistent with the DM constraints can be identified in this figure. The region at $M_2 \sim m_Z \sim m_h$ corresponds to the s-channel exchange of an almost on-shell Higgs or Z boson. Note that when $2\,m_{\chi_1^0}$ is too close to the Higgs or Z mass pole, the

JHEP08(2009)053

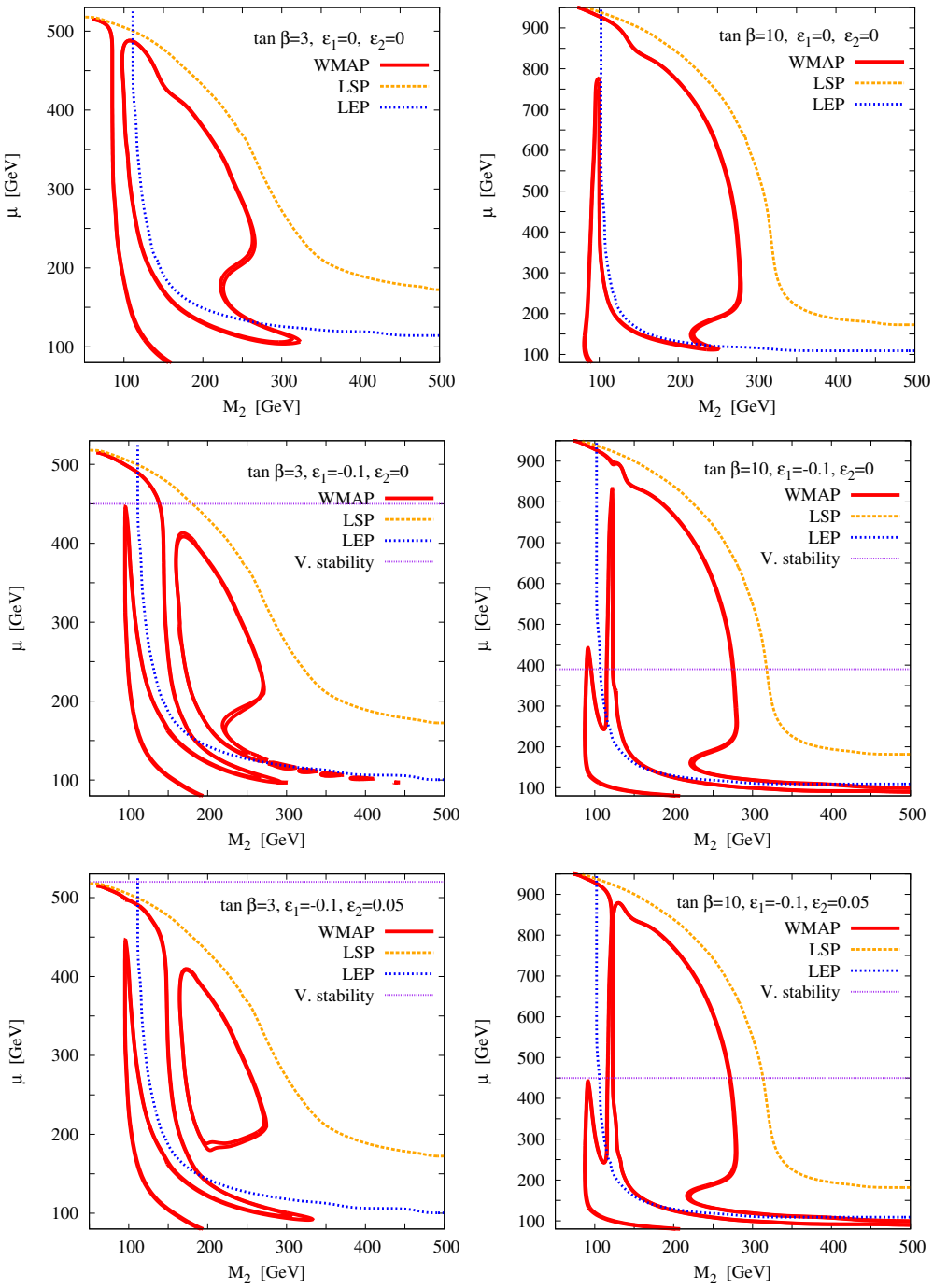

Figure 2. Regions of the $[M_2,\ \mu]$ plane in which the WMAP constraint is fulfilled (between the solid red lines). We use the parameter set described in the text, and values of $\tan\beta$, ϵ_1 and ϵ_2 as indicated in the various panels. The region above and to the right of the orange dashed curve corresponds to a stop LSP. The region to the left and below the blue dotted curve is excluded by direct chargino searches. Most of the region above the horizontal dashed line is excluded by vacuum instability.

JHEP08(2009)053

LSP annihilation is too efficient and leads to a much too small $\Omega_{\rm DM}\,h^2$. In any case, for the Higgs mass values obtained here, $m_h \sim 85(98)\,\text{GeV}$ for $\tan\beta = 3(10)$, this region is already excluded by the negative searches for chargino pairs at LEP2.

The region close to $M_2 \sim \mu \sim 200\,\text{GeV}$ corresponds to the LSP being a bino-higgsino mixture with sizeable couplings to W, Z and Higgs bosons, allowing for reasonably large rates for neutralino annihilation into $\chi_1^0\chi_1^0 \to W^+W^-$, ZZ, hZ and hh final states. Above and below the band, the LSP couplings to the various final states are either too strong or too weak to generate the relevant relic density.

Finally, for larger μ values, in the region close to the orange curve, the mass of the lightest neutralino approaches the mass of the lightest stop leading to an enhanced co-annihilation cross-section: $\chi_1^0\,\tilde{t}_1 \to W^+\,b,\,g\,t$ ($\sim 90\%$). Also, to a lesser extent ($\sim 5\%$), the annihilation cross-section of the stop NLSP contributes to the total cross-section by the process $\tilde{t}_1\,\tilde{t}_1 \to g\,g$.

Next we consider the $\epsilon_1 = -0.1$ case (the two middle panels). The features of the DM allowed regions are similar to the previous case. The main difference comes from the important enhancement of the Higgs mass due to the presence of the BMSSM operators. In this case it is possible to disentangle the Z and the h peaks, since the Higgs-related peak moves to higher M_2 values, due to the increase of the Higgs mass: $m_h = 122(150)\,\text{GeV}$ for $\tan\beta = 10(3)$. Furthermore, the latter peak is no longer excluded by chargino searches.

For large values of the μ parameter, the BMSSM operators destabilize the scalar potential. The regions above the horizontal dashed lines in figure 2 exhibit a metastable electroweak vacuum, following from the violation of eq. (4.4) which requires $\mu \lesssim m_A$. Similarly to the situation in the previous section, points right above the approximate analytical stability line may still be acceptable, as the stability constraint is somewhat alleviated by quantum corrections. However, with stop parameters as specified, computing the tunneling action for the middle and lower right panels reveals that the limit dictated by eq. (4.4) is in fact accurate to better than 15%. Hence a significant portion of the parameter space in the middle and lower right panels is indeed excluded by stability considerations.

The role of ϵ_2 can be seen from the lower two panels. It alleviates the stability constraint and slightly increases the Higgs mass. The ϵ_2-related effect on the Higgs mass is suppressed by $\tan^2\beta$ and consequently it is much more pronounced in the $\tan\beta = 3$ case than in the $\tan\beta = 10$ case.

5 The EWPT in the BMSSM

To study the electroweak phase transition, we analyze the finite temperature effective potential at two-loop order for the light scalar field. Detailed analyses for the case of the MSSM have been performed in refs. [28–31]. Here we focus on the region of parameter space of large m_A, for which there is a single light Higgs field at the phase transition. We review the main effects found in ref. [8] and study in more detail the interplay between the relevant parameters. We write the effective potential at finite temperature as follows:

$$V_{\rm eff}(\phi, T) = \frac{T^2\phi^2}{2}\left[\gamma - B\ln\left(\frac{\phi}{T}\right)\right] - \frac{m^2}{2}\phi^2 - ET\phi^3 + \frac{\lambda}{2}\phi^4. \tag{5.1}$$

The leading contributions to the γ-term and the E-term arise at one-loop. The γ-term is further corrected at two-loops by the so-called D_{SV} and D_{SS} terms [28]. The B-term contains the dominant two-loop corrections in the MSSM, which arise from the D_{SSV} and D_{SSS} diagrams that contribute with a logarithmic dependence [28]. For the numerical analysis we keep, in addition to the SM contributions, all contributions associated with the light right-handed stop. When considering a light left-handed stop, the relevant, dominant two-loop (order $g_s^2 h_t^2$ and h_t^4) corrections are added as well.

The strength of the phase transition is determined by the order parameter which, at the critical temperature of the phase transition T_c, is given by

$$\frac{\phi(T_c)}{T_c} = \frac{E}{2\lambda} + \frac{1}{2}\left(\frac{E^2}{\lambda^2} + \frac{2B}{\lambda}\right)^{1/2} \approx \frac{E}{\lambda}\left(1 + \frac{\lambda B}{E^2}\right). \tag{5.2}$$

We now discuss the various relevant parameters (E, B, λ) and their dependence on the MSSM parameters.

The cubic term arises in the regime for which the high temperature expansion of the bosonic one-loop contribution to the effective potential is valid. We write

$$E = E_{\rm SM} + E_{\rm MSSM}. \tag{5.3}$$

The SM contribution is given by

$$E_{\rm SM} = \frac{2m_W^3 + m_Z^3}{6\pi v^3}. \tag{5.4}$$

The dominant MSSM contribution comes from the stops (we provisionally neglect the $\tilde{t}_L - \tilde{t}_R$ mixing):

$$\delta V = -\frac{2N_c T}{12\pi}\left(m_{\tilde{t}_L}^3(T) + m_{\tilde{t}_R}^3(T)\right). \tag{5.5}$$

The finite temperature stop masses are given by

$$\begin{aligned} m_{\tilde{t}_L}^2(T) &= m_Q^2 + \frac{1}{2}h_t^2 s_\beta^2 \phi^2 + \frac{1}{8}g^2 c_{2\beta}\phi^2 + \alpha_L T^2, \\ m_{\tilde{t}_R}^2(T) &= m_U^2 + \frac{1}{2}h_t^2 s_\beta^2 \phi^2 + \alpha_R T^2, \end{aligned} \tag{5.6}$$

where we neglect contributions from the $\mathrm{U}(1)_Y$ gauge bosons in the field dependent terms. To maximize the value of $E_{\rm MSSM}$, one would like to take negative values of m_Q^2 and m_U^2,

$$m_Q^2 = -\alpha_L T^2, \qquad m_U^2 = -\alpha_R T^2, \tag{5.7}$$

that would cancel the thermal masses, yielding a purely cubic form in ϕ [29]:

$$E_{\rm MSSM}^{\rm max} = \frac{N_c}{3\pi} h_t^3 s_\beta^3. \tag{5.8}$$

Eq. (5.8) illustrates the effect of the stops and gives, to leading order, what would be an upper bound on the strength of the phase transition for the MSSM. It is impossible, however, to make the selection (5.7) simultaneously for both stops, due to constraints from the ρ parameter and the experimental bound on the sbottom mass (through its dependence on m_Q).

JHEP08(2009)053

The two-loop stop contribution to the finite temperature potential, which can increase $\phi(T_c)$ via its effect on B, is given by

$$\delta V = -\frac{g_s^2(N_c^2-1)T^2}{16\pi^2}\left[m_{\tilde{t}_L}^2(T)\log\frac{2m_{\tilde{t}_L}(T)}{3T}+m_{\tilde{t}_R}^2(T)\log\frac{2m_{\tilde{t}_R}(T)}{3T}\right]. \tag{5.9}$$

The effect is maximal when the limit of eq. (5.7) is realized:

$$B_{\rm stops}^{\rm max} = \frac{g_s^2 g_W^2 m_t^2}{\pi^2 m_W^2}. \tag{5.10}$$

Other logarithmic terms tend to diminish the value of B [28]. Note, however, that the net two-loop contributions to eq. (5.2) is the same when considering the maximal contributions from both stops or from a single one of them.

The strength of the phase transition is further affected by the quartic coupling λ. At zero temperature, it is related to the Higgs mass via $m_h^2 = \lambda_{\rm eff} v^2$, where

$$m_h^2 = m_Z^2 c_{2\beta}^2 - 16v^2\epsilon_1\cot\beta + \frac{3}{4\pi^2}m_t^2 h_t^2 \ln\frac{m_{\tilde{t}_L}m_{\tilde{t}_R}}{m_t^2}. \tag{5.11}$$

Eq. (5.11) is valid for large m_A and large $\tan\beta$. It includes the leading one-loop corrections. The ϵ_2 dependence is dropped. Adding in the leading finite temperature correction, we have

$$\lambda(T) = \lambda_{\rm eff} + \frac{3}{4\pi^2}h_t^4 s_\beta^4 \ln 2. \tag{5.12}$$

Thus, we can estimate,

$$\frac{\phi_c}{T_c} = \frac{v^2(E_{\rm SM}+E_{\rm MSSM})}{m_h^2 + 3(\ln 2)h_t^2 s_\beta^2 m_t^2/4\pi^2} \tag{5.13}$$

We now consider three specific cases. We use different values of the non-renormalizable contribution (ϵ_1) and the loop contribution ($m_{\tilde{t}_L}m_{\tilde{t}_R}$), but in such a way that m_h is fixed at the experimental lower bound.

(a) $m_h^{\rm tree} = 114\,$GeV. To keep $m_h = 114\,$GeV (and by that minimize the denominator of eq. (5.13)), we need the loop correction of the Higgs boson mass to vanish, namely

$$m_{\tilde{t}_L}m_{\tilde{t}_R} = m_t^2. \tag{5.14}$$

This constrains the possible values of $m_{\tilde{t}_L}^2(T)$ and $m_{\tilde{t}_R}^2(T)$, and gives the largest possible contribution to $E_{\rm MSSM}$ and to B, thus maximizing the strength of the phase transition. Smaller values of $m_{\tilde{t}_L}m_{\tilde{t}_R}$ are not allowed due to the experimental bound on m_h. Larger values are allowed but lead to a decrease in the numerator and an increase in the denominator in eq. (5.13).

The left panel of figure 3 shows the contour of $\phi_c/T_c = 1$ and the contour of $m_h = 114$ in the $m_{\tilde{t}_L}$-$m_{\tilde{t}_R}$ plane. We also show the curve of $m_{\tilde{t}_L} \gtrsim 175\,$GeV, corresponding to the experimental lower bound on $m_{\tilde{b}_L}$. We use $\tan\beta = 5$ and $\epsilon_1 = -0.065$, so that we obtain $m_h^{\rm tree} = 114\,$GeV. The m_h curve then corresponds to eq. (5.14). The plot shows the approximate symmetry in this case between $m_{\tilde{t}_L}$ and $m_{\tilde{t}_R}$, which is broken only by effects arising from D-terms. The allowed region is to the left of the $\phi_c/T_c = 1$ curve and above the $m_h = 114\,$GeV curve.

JHEP08(2009)053

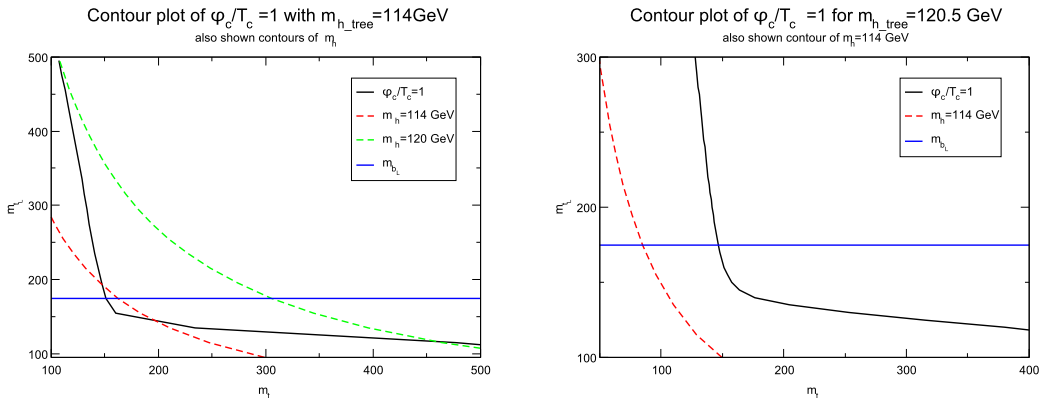

Figure 3. Contour of $\phi_c/T_c = 1$ (solid black curve), and contours of m_h (dashed curves) for $\tan\beta = 5$, and $\epsilon_1 = -0.065$ (left panel) or -0.08 (right panel). Also shown is the constraint arising from the lower bound on $m_{\tilde{b}_L}$ (solid blue line).

(b) $m_h^{\rm tree} > 114\,$GeV. Here we take values of ϵ_1 such that $m_h^{\rm tree} > 114\,$GeV. In this case, $m_{\tilde{t}_L} m_{\tilde{t}_R} < m_t^2$ is allowed. Such values further increase $E_{\rm MSSM}$ with respect to the values presented in case **(a)**, and the allowed region for a strong enough phase transition is increased, although here the sbottom mass constraint eliminates a large portion of this region. The right panel of figure 3 shows the $\phi_c/T_c = 1$ the $m_h = 114\,$GeV contours for this case.

(c) $m_h^{\rm tree} < 114\,$GeV. This is reminiscent of the usual MSSM results for the electroweak phase transition, in which one requires $m_{\tilde{t}_L}$ to be large enough to satisfy the $m_h^{\rm exp}$ value. The effect on $E_{\rm MSSM}$ is to effectively screen the contribution from the left-handed stop, thus reducing the cubic term to be smaller than half its maximum value and, furthermore, reducing the value of B. Variations in the value of m_Q produce only small variations in the value of m_U, as the main effect of increasing m_Q is to increase the one-loop value of the Higgs boson mass, thus reducing the strength of the phase transition. To compensate for that, a slightly smaller value of $m_{\tilde{t}_R}$ must be taken to increase $E_{\rm MSSM}$.

In the region of the parameter space where the EWPT is strong enough, a minimum where colour is broken might develop [29]. If the temperature where this minimum becomes as low as the potential at the origin, T_c^U, is higher than the critical temperature for the EWPT, T_c^ϕ, then the Universe is likely to end up in the colour breaking minimum. Thus, this region is excluded [32]. When the two stops are light enough, T_c^ϕ is safely higher than T_c^U. However, when we consider higher and higher values of $m_{\tilde{t}_L}$, and correspondingly, to keep the EWPT strong enough, lower and lower values of $m_{\tilde{t}_R}$, the closer do T_c^ϕ and T_c^U get to each other, until, at some critical values of $(m_{\tilde{t}_L}^c, m_{\tilde{t}_R}^c)$, we reach $T_c^\phi = T_c^U$.

Up to this point, we fixed the values of ϵ_1 and $\tan\beta$ and obtained the allowed regions in the $[m_{\tilde{t}_R}, m_{\tilde{t}_L}]$ plane. We learned that the presence of $\epsilon_1 = \mathcal{O}(-0.1)$ opens new regions in this plane where both the m_h constraint and the EWPT constraint are satisfied. We now turn our attention to the dependence on the other relevant parameters. More concretely, we fix $m_{\tilde{t}_L} = 200\,$GeV, which is close to the lowest value allowed by the $\delta\rho$ parameter, and obtain the dependence of ϕ_c/T_c and of m_h on $\tan\beta, m_{\tilde{t}_R}$, and ϵ_1.

JHEP08(2009)053

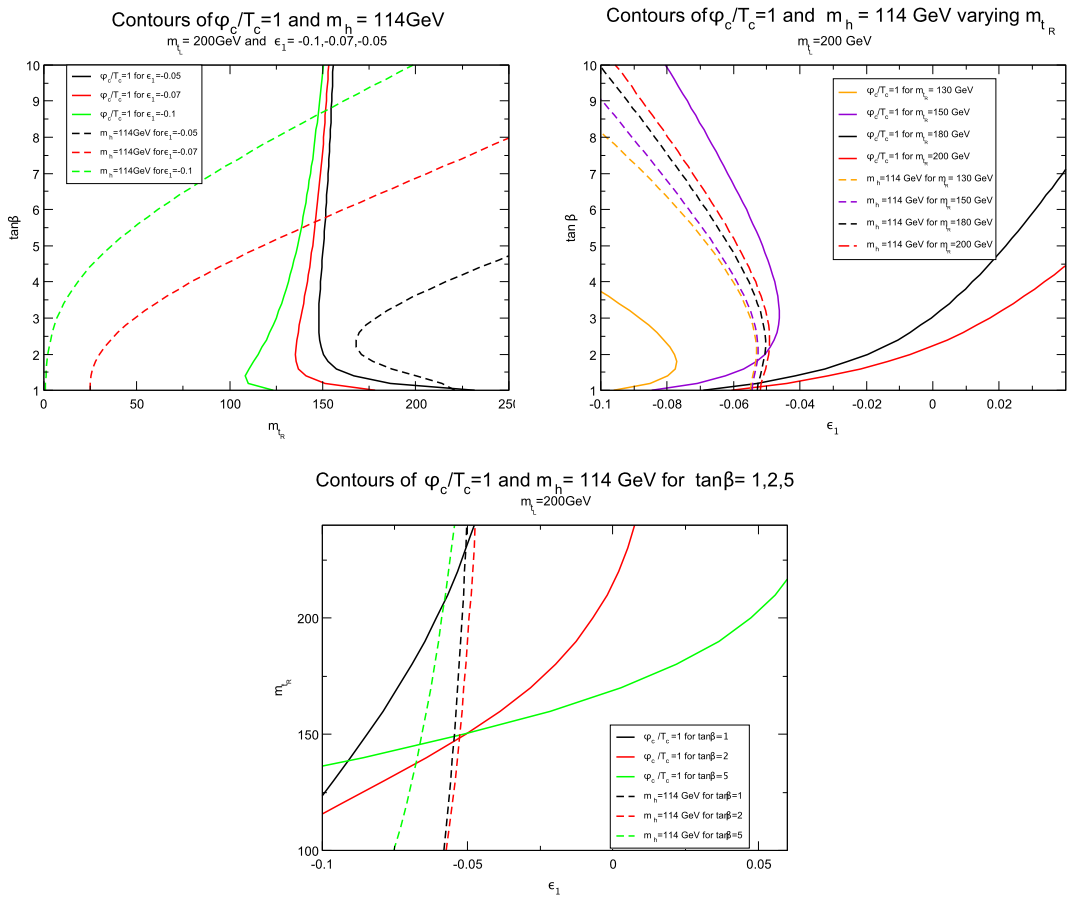

Figure 4. The dependencies of the Higgs mass and the EWPT on $\tan\beta$, $m_{\tilde{t}_R}$, and ϵ_1. We fix $m_{\tilde{t}_L} = 200\,\text{GeV}$. Solid lines indicate contours of $\phi_c/T_c = 1$ and dashed lines contours of $m_h = 114\,\text{GeV}$. Each same-colour pair of (solid and dashed) lines corresponds to the same set of parameters.

Our results are presented in figures 4 as contours of ϕ_c/T_c and of m_h in various parameter planes. In the top left panel we make discrete choices of ϵ_1, and present the results in the $[m_{\tilde{t}_R}, \tan\beta]$ plane. For each value of ϵ_1, the allowed region is to the right of the $m_h = 114\,\text{GeV}$ and to the left of the $\phi_c/T_c = 1$ curve. In the top right panel we make discrete choices of $m_{\tilde{t}_R}$ and present the results in the $[\epsilon_1, \tan\beta]$ plane. For each value of $m_{\tilde{t}_R}$, the allowed region is to the left of the $m_h = 114\,\text{GeV}$ and to the right of the $\phi_c/T_c = 1$ curve. In the lower panel we make discrete choices of $\tan\beta$ and present the results in the $[\epsilon_1, m_{\tilde{t}_R}]$ plane. For each value of $\tan\beta$, the allowed region is to the left of the $m_h = 114\,\text{GeV}$ and below and to the right of the $\phi_c/T_c = 1$ curve. We learn that small values of $\tan\beta$ are allowed and, furthermore, values of $m_{\tilde{t}_R} > m_t$ can simultaneously satisfy the requirement for baryogenesis and the Higgs boson mass bound.

To summarize the results depicted in figures 3 and 4, the BMSSM framework introduces the following significant differences with respect to the standard MSSM case:

1. The Higgs boson mass constraint decouples from the value of m_Q in some regions of parameter space. Consequently, a very light left-handed stop can contribute signifi-

JHEP08(2009)053

cantly to the cubic term in the effective potential. Explicitly, values of $m_{\tilde{t}_L} \lesssim 175\,\mathrm{GeV}$ ($m_Q \sim 0$) are now allowed, compared to the values of $m_Q \sim 2-3\,\mathrm{TeV}$, that are required in the MSSM.

2. The lowest allowed value for $m_{\tilde{t}_L}$ arises from electroweak precision measurements and from direct searches. For the MSSM, these constraints are superseded by requiring $m_h > 114\mathrm{GeV}$.

3. In the MSSM, a large value of left-right mixing in the stop sector is strongly favored. This is not necessary within the BMSSM. The actual consequences of left-right mixing in the stop sector are quite similar between the BMSSM and the MSSM: The Higgs boson mass is increased, which, in turn, weakens the phase transition (although this can be compensated by changing ϵ_1). Moreover, the contributions to the cubic term in the potential from the stops are screened, again weakening the phase transition.

4. Larger values of $m_{\tilde{t}_R}$ are allowed. Actually, the experimental bounds on the masses of the left handed squarks determine the largest possible mass of the right-handed stop.

5. Smaller values of $\tan\beta$ are now feasible.

We learn that the greater freedom in the values of the different parameters that affect the Higgs boson mass — $\tan\beta$, $m_{\tilde{t}_L}$, $m_{\tilde{t}_R}$ — implies that the allowed regions are similar to those identified in the early analyses of the EWPT [30].

Two final comments are in order. First, note that the inclusion of non-renormalizable operators of dimension six could modify the results. In particular, it is clear that for large m_A, such terms can induce additional contributions like those identified in ref. [33]. Vacuum stability considerations must be carefully taken into account in this case.

Second, as pointed out in refs. [5, 8], the non-renormalizable operators can induce new sources of CP violation in the scalar Higgs sector, that would modify the production mechanism of the baryon asymmetry of the Universe. These new sources could provide a relief to the tension between the large phases required to produce the BAU and the contributions to the electric dipole moments. Additionally, even in the absence of CP violation in the scalar Higgs sector, modifications to the EDMs arise from the new interaction terms between the Higgs bosons and the higgsinos [4]. These issues will be further studied elsewhere.

6 Conclusions

The main motivation to add non-renormalizable operators to the MSSM Higgs sector is to reduce the fine-tuning that is required by the lower bound on the Higgs mass. We have shown that, in addition, these operators have implications for cosmology that are very welcome: Regions of the supersymmetric parameter space that are favored by the dark matter constraints and by the requirement for a strong first-order electroweak phase transition, but are excluded within the MSSM, become viable within the BMSSM.

As concerns dark matter, a particularly important feature of the BMSSM is that the bulk region, for which the LSP is mostly bino-like and the sfermions are relatively light,

JHEP08(2009)053

can provide the adequate contribution to the energy density of the Universe while still satisfying the collider constraints on the Higgs boson as well as on the supersymmetric particle spectrum. Light stops co-annihilating with the LSP could have been active players in driving the dark matter relic density to its present value. It is also possible that nearly resonant LSP annihilation proceeded through exchange of the lightest Higgs particle itself.

If light stops are indeed found in upcoming experiments, large BMSSM corrections will be implied. In this scenario, parameter regions where μ is large (exhibiting some heavy neutralinos and charginos) will be significantly constrained by the requirement of vacuum stability.

As concerns the electroweak phase transition, the BMSSM has a dramatic effect when determining the range of parameters for which the phase transition is sufficiently strong to suppress sphaleron transitions in the broken phase. The fact that large stop-related radiative corrections to the Higgs mass are not required, allows light stop degrees of freedom to affect the dynamics of the phase transition by enhancing their contributions to the magnitude of the order parameter at the critical temperature.

Note added. Upon completion of this work, a related paper [34] has appeared. Where the two analyses overlap, we confirm their results.

Acknowledgments

We thank Cedric Delaunay for useful discussions. Results from this work were presented at the Planck 2009 conference in May 2009. The work of YN is supported by the Israel Science Foundation (ISF) under grant No. 377/07, the United States-Israel Binational Science Foundation (BSF), Jerusalem, the German-Israeli foundation for scientific research and development (GIF), and the Minerva Foundation. The work of ML was supported in part by Colciencias under contract 11150333018739. NB thanks an ESR position of the EU project RTN MRTN-CT-2006-035505 HEPTools. The work of NB and ML was supported in part by the Ecos-Nord program.

References

[1] A. Strumia, *Bounds on Kaluza-Klein excitations of the SM vector bosons from electroweak tests*, *Phys. Lett.* **B 466** (1999) 107 [hep-ph/9906266] [SPIRES].

[2] A. Brignole, J.A. Casas, J.R. Espinosa and I. Navarro, *Low-scale supersymmetry breaking: effective description, electroweak breaking and phenomenology*, *Nucl. Phys.* **B 666** (2003) 105 [hep-ph/0301121] [SPIRES].

[3] J.A. Casas, J.R. Espinosa and I. Hidalgo, *The MSSM fine tuning problem: a way out*, *JHEP* **01** (2004) 008 [hep-ph/0310137] [SPIRES].

[4] M. Pospelov, A. Ritz and Y. Santoso, *Flavor and CP violating physics from new supersymmetric thresholds*, *Phys. Rev. Lett.* **96** (2006) 091801 [hep-ph/0510254] [SPIRES]; *Sensitivity to new supersymmetric thresholds through flavour and CP violating physics*, *Phys. Rev.* **D 74** (2006) 075006 [hep-ph/0608269] [SPIRES].

[5] M. Dine, N. Seiberg and S. Thomas, *Higgs physics as a window beyond the MSSM (BMSSM)*, *Phys. Rev.* **D 76** (2007) 095004 [arXiv:0707.0005] [SPIRES].

JHEP08(2009)053

[6] P. Batra and E. Ponton, *Supersymmetric electroweak symmetry breaking*, *Phys. Rev.* **D 79** (2009) 035001 [arXiv:0809.3453] [SPIRES].

[7] I. Antoniadis, E. Dudas, D.M. Ghilencea and P. Tziveloglou, *MSSM with dimension-five operators ($MSSM_5$)*, *Nucl. Phys.* **B 808** (2009) 155 [arXiv:0806.3778] [SPIRES].

[8] K. Blum and Y. Nir, *Beyond MSSM baryogenesis*, *Phys. Rev.* **D 78** (2008) 035005 [arXiv:0805.0097] [SPIRES].

[9] K. Cheung, S.Y. Choi and J. Song, *Impact on the light Higgsino-LSP scenario from physics beyond the minimal supersymmetric standard model*, *Phys. Lett.* **B 677** (2009) 54 [arXiv:0903.3175] [SPIRES].

[10] G.L. Kane, T.T. Wang, B.D. Nelson and L.-T. Wang, *Theoretical implications of the LEP Higgs search*, *Phys. Rev.* **D 71** (2005) 035006 [hep-ph/0407001] [SPIRES];
M. Drees, *A supersymmetric explanation of the excess of Higgs-like events at LEP*, *Phys. Rev.* **D 71** (2005) 115006 [hep-ph/0502075] [SPIRES];
S.G. Kim et al., *A solution for Little hierarchy problem and $b \to s\gamma$*, *Phys. Rev.* **D 74** (2006) 115016 [hep-ph/0609076] [SPIRES];
A. Belyaev, Q.-H. Cao, D. Nomura, K. Tobe and C.P. Yuan, *Light MSSM Higgs boson scenario and its test at hadron colliders*, *Phys. Rev. Lett.* **100** (2008) 061801 [hep-ph/0609079] [SPIRES];
R. Essig, *Implications of the LEP Higgs bounds for the MSSM stop sector*, *Phys. Rev.* **D 75** (2007) 095005 [hep-ph/0702104] [SPIRES].

[11] D. Hooper and T. Plehn, *Dark matter and collider phenomenology with two light supersymmetric Higgs bosons*, *Phys. Rev.* **D 72** (2005) 115005 [hep-ph/0506061] [SPIRES];
M. Asano, S. Matsumoto, M. Senami and H. Sugiyama, *Neutralino dark matter in light Higgs boson scenario*, *Phys. Lett.* **B 663** (2008) 330 [arXiv:0711.3950] [SPIRES];
S.G. Kim, N. Maekawa, K.I. Nagao, K. Sakurai and T. Yoshikawa, *Neutralino dark matter in minimal supersymmetric standard model with natural light Higgs sector*, *Phys. Rev.* **D 78** (2008) 075010 [arXiv:0804.3084] [SPIRES].

[12] N. Arkani-Hamed, A. Delgado and G.F. Giudice, *The well-tempered neutralino*, *Nucl. Phys.* **B 741** (2006) 108 [hep-ph/0601041] [SPIRES].

[13] WMAP collaboration, J. Dunkley et al., *Five-year Wilkinson Microwave Anisotropy Probe (WMAP) observations: likelihoods and parameters from the WMAP data*, *Astrophys. J. Suppl.* **180** (2009) 306 [arXiv:0803.0586] [SPIRES].

[14] Planck collaboration, F.R. Bouchet, *The Planck satellite: status & perspectives*, *Mod. Phys. Lett.* **A 22** (2007) 1857 [SPIRES].

[15] G. Bélanger, F. Boudjema, A. Pukhov and A. Semenov, *MicrOMEGAs2.0: a program to calculate the relic density of dark matter in a generic model*, *Comput. Phys. Commun.* **176** (2007) 367 [hep-ph/0607059] [SPIRES]; *Dark matter direct detection rate in a generic model with MicrOMEGAs2.1*, *Comput. Phys. Commun.* **180** (2009) 747 [arXiv:0803.2360] [SPIRES].

[16] A. Djouadi, J.-L. Kneur and G. Moultaka, *SuSpect: a Fortran code for the supersymmetric and Higgs particle spectrum in the MSSM*, *Comput. Phys. Commun.* **176** (2007) 426 [hep-ph/0211331] [SPIRES].

[17] S. Davidson, T. Falk and M. Losada, *Dark matter abundance and electroweak baryogenesis in the CMSSM*, *Phys. Lett.* **B 463** (1999) 214 [hep-ph/9907365] [SPIRES].

JHEP08(2009)053

[18] C. Balázs, M.S. Carena and C.E.M. Wagner, *Dark matter, light stops and electroweak baryogenesis*, *Phys. Rev.* **D 70** (2004) 015007 [hep-ph/0403224] [SPIRES].

[19] C. Balázs, M.S. Carena, A. Menon, D.E. Morrissey and C.E.M. Wagner, *The supersymmetric origin of matter*, *Phys. Rev.* **D 71** (2005) 075002 [hep-ph/0412264] [SPIRES].

[20] A.H. Chamseddine, R.L. Arnowitt and P. Nath, *Locally supersymmetric grand unification*, *Phys. Rev. Lett.* **49** (1982) 970 [SPIRES];
R. Barbieri, S. Ferrara and C.A. Savoy, *Gauge models with spontaneously broken local supersymmetry*, *Phys. Lett.* **B 119** (1982) 343 [SPIRES];
L.J. Hall, J.D. Lykken and S. Weinberg, *Supergravity as the messenger of supersymmetry breaking*, *Phys. Rev.* **D 27** (1983) 2359 [SPIRES];
N. Ohta, *Grand unified theories based on local supersymmetry*, *Prog. Theor. Phys.* **70** (1983) 542 [SPIRES].

[21] M. Drees and M.M. Nojiri, *Neutralino relic density in minimal $N = 1$ supergravity*, *Phys. Rev.* **D 47** (1993) 376 [hep-ph/9207234] [SPIRES].

[22] A. Djouadi, M. Drees and J.L. Kneur, *Neutralino dark matter in mSUGRA: reopening the light Higgs pole window*, *Phys. Lett.* **B 624** (2005) 60 [hep-ph/0504090] [SPIRES].

[23] K. Blum, C. Delaunay and Y. Hochberg, *Vacuum (meta)stability beyond the MSSM*, arXiv:0905.1701 [SPIRES].

[24] A. Belyaev, S. Dar, I. Gogoladze, A. Mustafayev and Q. Shafi, *Interplay of Higgs and sparticle masses in the CMSSM with updated SUSY constraints*, arXiv:0712.1049 [SPIRES].

[25] K. Griest and D. Seckel, *Three exceptions in the calculation of relic abundances*, *Phys. Rev.* **D 43** (1991) 3191 [SPIRES].

[26] J.R. Ellis, K.A. Olive and Y. Santoso, *Calculations of neutralino-stop coannihilation in the CMSSM*, *Astropart. Phys.* **18** (2003) 395 [hep-ph/0112113] [SPIRES].

[27] Particle Data Group collaboration, C. Amsler et al., *Review of particle physics*, *Phys. Lett.* **B 667** (2008) 1 [SPIRES].

[28] J.R. Espinosa, *Dominant two-loop corrections to the MSSM finite temperature effective potential*, *Nucl. Phys.* **B 475** (1996) 273 [hep-ph/9604320] [SPIRES].

[29] M.S. Carena, M. Quirós and C.E.M. Wagner, *Opening the window for electroweak baryogenesis*, *Phys. Lett.* **B 380** (1996) 81 [hep-ph/9603420] [SPIRES].

[30] A. Brignole, J.R. Espinosa, M. Quirós and F. Zwirner, *Aspects of the electroweak phase transition in the minimal supersymmetric standard model*, *Phys. Lett.* **B 324** (1994) 181 [hep-ph/9312296] [SPIRES].

[31] J.R. Espinosa, M. Quirós and F. Zwirner, *On the electroweak phase transition in the minimal supersymmetric standard model*, *Phys. Lett.* **B 307** (1993) 106 [hep-ph/9303317] [SPIRES];
J.R. Espinosa, *Dominant two-loop corrections to the MSSM finite temperature effective potential*, *Nucl. Phys.* **B 475** (1996) 273 [hep-ph/9604320] [SPIRES];
M.S. Carena, M. Quirós and C.E.M. Wagner, *Opening the window for electroweak baryogenesis*, *Phys. Lett.* **B 380** (1996) 81 [hep-ph/9603420] [SPIRES];
D. Delepine, J.M. Gerard, R. Gonzalez Felipe and J. Weyers, *A light stop and electroweak baryogenesis*, *Phys. Lett.* **B 386** (1996) 183 [hep-ph/9604440] [SPIRES];
J.M. Cline and K. Kainulainen, *Supersymmetric electroweak phase transition: beyond perturbation theory*, *Nucl. Phys.* **B 482** (1996) 73 [hep-ph/9605235] [SPIRES];

JHEP08(2009)053

M. Losada, *High temperature dimensional reduction of the MSSM and other multi-scalar models*, *Phys. Rev.* **D 56** (1997) 2893 [hep-ph/9605266] [SPIRES];
M. Laine, *Effective theories of MSSM at high temperature*, *Nucl. Phys.* **B 481** (1996) 43 [*Erratum ibid.* **B 548** (1999) 637] [hep-ph/9605283] [SPIRES];
G.R. Farrar and M. Losada, *SUSY and the electroweak phase transition*, *Phys. Lett.* **B 406** (1997) 60 [hep-ph/9612346] [SPIRES];
D. Bödeker, P. John, M. Laine and M.G. Schmidt, *The 2-loop MSSM finite temperature effective potential with stop condensation*, *Nucl. Phys.* **B 497** (1997) 387 [hep-ph/9612364] [SPIRES];
B. de Carlos and J.R. Espinosa, *The baryogenesis window in the MSSM*, *Nucl. Phys.* **B 503** (1997) 24 [hep-ph/9703212] [SPIRES];
M. Laine and K. Rummukainen, *The MSSM electroweak phase transition on the lattice*, *Nucl. Phys.* **B 535** (1998) 423 [hep-lat/9804019] [SPIRES];
M.S. Carena, M. Quirós and C.E.M. Wagner, *Electroweak baryogenesis and Higgs and stop searches at LEP and the Tevatron*, *Nucl. Phys.* **B 524** (1998) 3 [hep-ph/9710401] [SPIRES];
M. Losada, *The two-loop finite-temperature effective potential of the MSSM and baryogenesis*, *Nucl. Phys.* **B 537** (1999) 3 [hep-ph/9806519] [SPIRES];
M. Laine and K. Rummukainen, *Higgs sector CP violation at the electroweak phase transition*, *Nucl. Phys.* **B 545** (1999) 141 [hep-ph/9811369] [SPIRES];
M. Losada, *Mixing effects in the finite-temperature effective potential of the MSSM with a light stop*, *Nucl. Phys.* **B 569** (2000) 125 [hep-ph/9905441] [SPIRES];
M. Laine and M. Losada, *Two-loop dimensional reduction and effective potential without temperature expansions*, *Nucl. Phys.* **B 582** (2000) 277 [hep-ph/0003111] [SPIRES];
M. Carena, G. Nardini, M. Quirós and C.E.M. Wagner, *The baryogenesis window in the MSSM*, *Nucl. Phys.* **B 812** (2009) 243 [arXiv:0809.3760] [SPIRES].

[32] J.M. Cline, G.D. Moore and G. Servant, *Was the electroweak phase transition preceded by a color broken phase?*, *Phys. Rev.* **D 60** (1999) 105035 [hep-ph/9902220] [SPIRES].

[33] C. Grojean, G. Servant and J.D. Wells, *First-order electroweak phase transition in the standard model with a low cutoff*, *Phys. Rev.* **D 71** (2005) 036001 [hep-ph/0407019] [SPIRES].

[34] M. Berg, J. Edsjo, P. Gondolo, E. Lundstrom and S. Sjors, *Neutralino dark matter in BMSSM effective theory*, arXiv:0906.0583 [SPIRES].

JHEP08(2009)053